應用三維数值模式模擬浚渫渠道之泥砂管理技術

Reservoir management technique with the dredged guiding channel by employing a 3D-Numerical model

國立臺灣大學 土木工程學系 碩士生	國立臺灣大學水工 試驗所 專案計畫助理研究員	國立臺灣大學水工 試驗所研究員暨生 物環境系統工程學 系兼任教授	國立臺灣大學 工學院土木工 程學系 教授
Nafeela Imtiyaz	李豐佐 Fong-Zuo Lee	賴進松 Jihn-Sung Lai	林國峰 Gwo-Fong Lin

摘要

大壩和水庫為當今人類維持正常且穩定水資源供應的重要基礎設施，而水庫的維護與營運隨其扮演的功能特性而複雜程度不同，基本上，水庫可確保水、食物、能源及具備防洪功能，然而，水庫淤積問題對於水庫的水資源永續發展影響甚鉅，而水庫淤積的泥砂則主要來自於水庫集水區降下暴雨時，所夾帶的大量泥砂運移至水庫內所造成，若水庫進行排砂操作，則對下游河道產生生態問題，此外，若水庫缺水時，則可能造成農地無水可灌而休耕。為了處理水庫泥砂淤積的問題，可實施各種水庫泥砂管理策略，包含減少集水區的產砂量、減少入庫泥砂的沉積或是將淤積水庫的泥砂清除，其中，減少入庫泥砂的沉積為最有效益的防止泥砂淤積方式。因此，研究颱風豪雨時期，所引發的渾水流在水庫的運移型態，對於了解入庫泥砂淤積的行為非常重要，且可了解實施各種防淤策略組合或是實施前後的功效。本研究目的在於利用三維數值模式 ANSYS-CFX，模擬颱風豪雨時期入庫渾水流之運移型態，並了解利用浚渫所形成之庫底導流槽，對於曾文水庫各出水工之排砂效率影響。本研究利用實驗室水槽數據及物理模型試驗數據進行模式檢定和驗證，並針對重現期 100 年、5 年及 2 年的洪水事件，模擬通過所有出水工的排砂效率，根據模擬結果顯示其排砂效率分別為 27.03%、20.24% 和 38.26%，因此，從從研究結果可以得出以下結論，浚渫渠道的排砂效益取決於洪峰流量和洪水的持續時間，模擬結果亦顯示浚渫渠道內的渾水速度和濃度有增加的趨勢。

關鍵詞： 水庫淤積、渾水流、三維數值模式、排砂效率、浚渫渠道

Abstract

Sediment management in storage dam projects aims to ensure the long-term sustainability of facilities to store large amounts of water for consumption during droughts. With such type of storage, the floods can be attenuated as well. In order to manage the reservoir storage, three main strategies are usually practiced depending upon the feasibility, i.e., reduce the sediment yield from the watershed, route the incoming sediment and remove the deposited sediment (3 Rs). The sediment routing techniques have proven the most effective in reducing reservoir sedimentation and maintaining or re-establishing sediment continuity similar to pre-dam conditions. Studying the dynamics of approaching turbidity currents induced by heavy flooding during typhoon events is essential for understanding the factors influencing sedimentation in the reservoir system. It plays a crucial role in selecting and implementing management techniques in this system. These existing techniques can be modified and combined to build a single efficient approach to counteract reservoir sedimentation.

Zengwen reservoir, one of Taiwan's most important water resources, has been impacted by sedimentation; therefore, it has been chosen as a case study. The reservoir desilting strategy involving a dredged guiding channel of length 4.8 km and width 0.2 km is tested for flood events of three different return periods by employing a 3D-numerical model ANSYS-CFX 2020 R1. The effectiveness of the strategy is evaluated in terms of desilting efficiency. The numerical model is calibrated and validated using the laboratory flume data and physical model test results. The simulated results show the total increase in desilting efficiency through all outlets is 27.03 %, 20.24 %, and 38.26 % for a flood event of return periods hundred, five, and two, respectively. From the findings, it can be concluded that the desilting efficiency of the dredged guiding channel depends on the peak discharge and flood duration. The results also show an increase in the velocity and concentration within the dredged guiding channel. The results could allow water resource authorities to undertake desilting measures ahead of time before the occurrence of highly unstable flood events.

Keywords: Reservoir sedimentation; turbidity currents; 3D-numerical modelling; desilting efficiency; guiding channel

1. Introduction

1.1.Research motivation

According to Mahmood (1987), the global yearly loss of reservoir storage capacity was roughly 1%; the calculation was based on the existing data on reservoir sedimentation trapping rates. However, according to Wisser (2013), the average loss of storage capacity due to reservoir sedimentation has been reported to range between 0.5-1% per annum. Most dams are built with a 100-year life expectancy, implying they have enough dead storage capacity to keep them operational for 100 years while sediments gradually accumulate (Wieland et al. 2010). The issue of reservoir sedimentation has caused significant problems in many parts of the world, resulting in severe implications for water conservation, flood control, and energy production.

Reservoir sedimentation has been a problem for a very long time. Despite this, it got little to no attention in the early twentieth century. Therefore, no long-term solutions were devised during dam construction. According to Morris and Fan (1998), the four broad categories of management activities to address reservoir sedimentation are (1) techniques to reduce sediment inflow from upstream, (2) techniques to pass sediment through or around the reservoirs to minimize sediment accumulation (3) techniques to redistribute or remove sediment deposits, or (4) techniques to acclimate to sedimentation. Demolishing the existing dam to restore the reservoir's storage capacity and sediment balance is neither cost-effective nor environmentally sustainable. As a result, researchers will need to devise better and more effective management strategies to provide sufficient reservoir storage to combat major flooding and drought and ensure the sustainability of reservoirs. Due to turbidity currents created during typhoon occurrences, substantial sedimentation rates have been seen in the Zengwen reservoir. Therefore, finding a sustainable solution is the objective of this study that will help increase the venting efficiency of the turbidity currents in order to maintain the functioning of the reservoir.

1.2.Research purpose

The changing climate patterns have made natural disasters like floods and droughts very imminent in the Taiwan region. Taiwan receives 2500 mm of yearly precipitation on average. Due to Taiwan's fragile geological and hydrological characteristics a large amount of sediment flows into the reservoir from the watershed. As a result, we may argue that Taiwan's steep slopes have exacerbated the problem of reservoir sedimentation in several strategically vital areas Zengwen reservoir being one such crucial region.

Our research idea was based on the test of two techniques in integration, i.e., sediment routing and sediment removal, which we aimed to achieve by dredging and sediment venting. Even though the dredging operation is already active in the Zengwen Reservoir, we planned to dredge a channel of specific dimensions that will guide the turbidity currents generated during the typhoon events. We wanted to see how sediment removal will enhance the efficiency of sediment routing. By the end of the research, we were able to deduce a conclusion about the influence of the dredged channel on the venting efficiency of floods of different intensities. We chose the depth and length of the guiding channel based on the particle size analysis in the Zengwen reservoir. We constructed a dredged channel extending from A-01 to A-10 and five-meter in depth. Since our primary aim was to find a practical solution to tackle reservoir sedimentation, it was essential to find the dimensions for a channel that would be practical to dredge. However, the width of the dredging is not a problem in the Zengwen reservoir.

1.3.Previous studies on strategies to improve desilting efficiency

Hydrodynamic and sediment transport modeling is essential for the analysis of the process of aggradation and degradation in the river system, the sediment management in a reservoir, and the study of the downstream effect on the coastal sediment. Numerical models are devoid of scaling errors and allow for a detailed analysis of the entire flow field. They can be used to investigate the formation of a turbidity current at a reservoir's real site, which is usually impossible to replicate in detail in a laboratory (Wildt et al., 2020). To study flood-related problems, the numerical models generally employed are based on solving the 1-D or the 2-D Saint-Venant equations. Although for many applications, these models can reproduce reasonably well results but to provide accurate predictions, these models need to be calibrated quite accurately. In regions where 3-D effects (e.g., where strong vertical non-uniformity of the flow) become necessary for such cases, one should consider using 3-D numerical models in which the fundamental equations that govern fluid flows and sediment concentrations are the Reynolds-averaged Navier-Stokes (RANS) equations and the sediment transport equation. Wang et al., (2008) in their study have presented a three-dimensional hydrodynamic and sediment transport model which investigates the variation of sediment concentration in the Shihmen Reservoir in Taiwan under typhoon-induced flood events. The simulation outcome clearly reflects the three-dimensional feature of the velocity field in the reservoir; other results include the time variation of the velocity vectors and sediment concentration at selected vertical layers. Thus, reflecting the importance of 3D-modelling of the flow in the reservoirs. In the study conducted by Lee et al., (2014) the 3D-based CFX computational fluid dynamics model was applied to provide detailed numerical solutions for complex topography and structures. The simulated outflow concentration varying with time was predicted well to show good agreement with experimental data. In the research study of Heimsund et al., (2002) the CFD software Flow-3D was used to develop a 3D, fluid-dynamics model for the analysis of sediment transport, erosion and deposition by turbidity currents. Another such study of 3D numerical model using the CFX was constructed by A. Lavelli et al., (2002) to simulate turbidity currents in Lake Lugano, Switzerland. Cantero et al., (2003) study presents two and three-dimensional CFD simulations of a discontinuous density current, using a stabilized equal-order finite element method. Anastasios N. Georgoulas et al., (2010) made use of a commercial software FLUENT in order to simulate the 3D dynamics and flow behavior of turbidity currents. The purpose of the study was to justify the ability of the numerical model in capturing various essential characteristics of turbidity currents, such as their flow structure, the effect of suspended sediment mixture composition in their temporal as well as spatial evolution.

1.4. Study area

The Zengwen Dam, with a height of 134 meters and a length of 400 meters, is one of Taiwan's largest dams, impounding the country's largest reservoir by volume. The Zengwen Reservoir has a catchment area of 481 km^2. The Reservoir has a maximum daily inflow of 3.4 x 10^8 m^3 and an annual inflow of 1.74 x 10^9 m^3. The reservoir pool impounds roughly 15.1 km in length from the dam site to the Dapu-check Dam, the upstream barrier, with a normal water level of 227 m, forming a water surface area of 1.71 x 10^7 m^2. The outlets present in the reservoir are three spillways, one power plant intake (PPI), a permanent river outlet (PRO), and a desilting tunnel (the elephant trunk tunnel) with design discharge of 11345 m^3/sec, 56m^3/sec, 180 m^3/sec and 995 m^3/sec respectively.

The Zengwen reservoir catchment area is a part of the upper and middle reaches of the Zengwen watershed, with the highest elevation of 2160 m and the lowest elevation of 102 m at the dam site. However, high relief and steep gradient cause massive erosion of the riverbed. Therefore, the rivers flowing through the reservoir carry vast amounts of eroded sediment caused by a rapid movement of river over the steep riverbeds. Taiwan is widely regarded as having the highest sediment production in the world, owing to its steep topography, frequent tectonic activity, fragile geology, intense precipitation, and frequent typhoons (J.P. Liu et al., 2018). However, typhoon-induced landslides are the major cause of reservoir sedimentation.

Even though Taiwan receives 2500 mm of precipitation every year due to its southern Asian monsoon climate and extremely heavy rains during typhoons, it has been estimated that Taiwan can only accumulate water for 41 days (WRA, Taiwan). It implies a lack of storage facilities even though Taiwan has 18 major dams. Unfortunately, a considerable part of these reservoirs' active storage capacity has been lost to sedimentation.

On September 27–29, 2008, Typhoon Jangmi poured torrential rains throughout Taiwan, which had previously been hit hard by Typhoon Sinlaku in early September, making the storage capacity fall to 79% of the initial storage capacity. Generating a peak inflow discharge of 4424 m^3/s with hydrograph patterns similar to the inflow and water level variation, Jangmi poured 994 mm of rainfall in the Chiayi region (Lee et al., 2014).

However, typhoon Morakot was a destructive tropical typhoon that hit Taiwan from August 7 to 9, 2009. Typhoon Morakot wreaked havoc on Taiwan, pouring 2550 mm average rain in the Zengwen Reservoir watershed and generating 1,467 hectares of landslides. In addition to sediment, around 800,000 m^3 of material got accumulated on the upstream end over a distance of about 1 km; most of it was made up of logs and tree branches. The prolonged movement of Morakot during both the landfall and post-landfall phases contributed to the heavy rainfall. As a result, the reservoir's capacity was reduced by 91.08 Mm^3 (13 percent of its initial capacity). Also, a massive amount of silt and debris had deposited near the reservoir outlets, disrupting the functioning of the reservoir. The reservoir bed accumulated sediment up to 177 m, substantially higher than the intake's invert elevation (E.L.154 m), causing PRO to malfunction (Wang et al., 2018).

Therefore, to restore the lost capacity and remove the sediments near the outlets, a dredging operation was started in December 2012. It was the first dredging operation since the dam construction in 1973; the progress of the dredging operation over the years can be seen in figure 2. During dredging, the covered area was in the fan shape with a radius of 600 m and an angle of 120 degrees extending from the reservoir's intake gatehouse. The total dredged volume from 2012 to 2016 was 2.1 Mm^3. Further dredging was continued, and the amount dredged from 2016 to 2018 was 1.38 Mm^3. Additionally, in 2012 structural changes were performed, including refurbishment of the PRO by replacing the original valve with a jet flow gate, construction of maintenance tunnels, and a desilting tunnel (Wang et al., 2018).

However, with the anticipated average annual sediment inflow of 5.06Mm^3, it is clear that yearly dredging near the intake will not be able to sustain reservoir capacity. Due to the wide range of seasonal and annual rainfall in the catchment, reservoir sediment management is a complex issue in the Zengwen reservoir (Hsiao-Wen Wang et al., 2018). The average storage depletion is estimated to be 6593 x 10^3 m^3 which is 0.8% of the initial storage capacity of 748,400 x 10^3 m^3 (Taiwan Water Resources Agency (WRA)).

2. Methodology

2.1.Numerical model

The numerical model is based on the flow solver CFX from ANSYS-2020 R1. This 3D-based CFD model is applied and employed to obtain detailed numerical solutions for complex field topography and desilting structures. The solver CFX issued from ANSYS, Inc. allows the implementation of user programming and expert controls (De Cesare et al., 2001；Oehy and Schleiss, 2007；Chamoun et al.,2017). Suspended sediment concentration is conducted in the CFX formulas through its advection-diffusion model with a continuous and homogeneous Eulerian description. By solving mass balances of turbid water, momentum balance for the mixture accounts for the changing mixture density are considered on different mass fractions. Mass and momentum transfers from one phase to the other are neglected. The turbulent stresses are calculated with the k-epsilon turbulence model, which employs the eddy-viscosity hypothesis to introduce the momentum transportation of turbidity current. The method is isothermal and incompressible, which means that no heat transfer is considered, and hence no thermal energy balance is solved. The buoyancy effect is adapted through variable parameters. The fluid density is defined by the sediment mass fraction concentration, with the Reynolds-averaged Navier-Stokes equations serving as the basis for the computation. In this study, we also take fall velocity of the particles into account. The continuity equation (Eq. 1) and the momentum equation (Eq. 2), along with the (Eq. 3) for sediment concentration, are the governing equations for turbidity current movement.

$$\frac{\partial \rho}{\partial t}+\frac{\partial}{\partial x_i}(\rho U_i)=0 \tag{1}$$

$$\frac{\partial(\rho U_i)}{\partial t}+\frac{\partial(\rho U_i U_j)}{\partial x_j}=-\frac{\partial \rho'}{\partial x_i}+\frac{\partial}{\partial x_j}\left[\upsilon_{eff}\left(\frac{\partial U_i}{\partial x_j}+\frac{\partial U_j}{\partial x_i}\right)\right]+G'-w_f w_f\frac{\partial}{\partial x_i}\left(\frac{\rho_w \rho_s}{\rho}\right) \tag{2}$$

$$\frac{\partial(\rho c_p)}{\partial t}+\frac{\partial(\rho c_p(U_i))}{\partial t}=\frac{\upsilon_{eff}}{\sigma_p}c_p\left(\frac{\partial U_i}{\partial x_j}+\frac{\partial U_j}{\partial x_i}\right)-w_f\frac{\partial}{\partial x_i}\left(c_p\frac{\rho_w}{\rho}\right) \tag{3}$$

where, ρ = mixture density = $(1-c_p)\rho_w + c_p\rho_s$; c_p = sediment particle concentration; ρ_w = water density; ρ_s = particle density, t = time, $x_{i,j}$ = cartesian coordinates ≡ (x, y, z), $U_{i,j}$ = velocity components ≡ (u, v, w), p'= modified pressure, υ_{eff} = effective viscosity, $G'=\left[0,0,(\rho-\rho_w)g\right]$ is a buoyancy vector, w_f = fall velocity of particle, g= acceleration due to gravity, and σ_p = turbulent Prandtl number for the sediment concentration.

Where ν_{eff} is based on the eddy viscosity concept and similar to the zero-equation model as $\upsilon_{eff}=\upsilon+\upsilon_t$. Where ν is the kinematic viscosity of water and ν_t is the turbulence viscosity. The turbulence viscosity is linked to the turbulence kinetic energy and dissipation via the relation as $\upsilon_t=C_v\rho\frac{k^2}{\varepsilon}$. Where $C_v=0.09$ is a constant. In addition, we also considered νeff of the mixture by employing Van Rijn's (1987) equation for kinematic viscosity of a sediment-laden flow. Then, propose a new concept to decide effective viscosity as Eq. 4 using viscosity and sediment concentration.

$$\upsilon_{eff}=\min(\upsilon(1+\lambda)(1+0.5\lambda),5,\upsilon+\upsilon_t) \tag{4}$$

where, λ is used to develop a relationship between concentration and mixture viscosity as $\lambda = \left((a'/(0.73998c_p + 0.0001)^{\frac{1}{3}} - 1 \right)^{-1}$ where $\boldsymbol{a}$ is a viscosity coefficient.

Regarding fall velocity of particle, Rubey (1933) was the first to provide a formula for calculating fall velocities of gravel, sand, and silt particle. Many researchers have proposed a variety of semi-theoretical and empirical relationships for the sediment particle fall velocity since then. The fall velocity (or settling velocity) w_f in water with suspended sediment concentration C can be estimated using equation proposed by Richardson and Zaki (1954) as Eq. 5.

$$w_f = w_{tf}\left(1 - c_p\right)^m \tag{5}$$

where w_{tf} is the terminal fall velocity of particle in a clear water and m is a Reynolds number (Re) dependent coefficient. Camenen (2007) and Zhiyao et al., (2008) proposed an equation for w_{tf} in clear water and obtained the following formula which has been used in this study.

$$w_{tf} = \frac{\upsilon}{d} d_*^3 \left[38.1 + 0.93 d_*^{\frac{12}{7}} \right]^{-\frac{7}{8}} \tag{6}$$

where, $d_* = \left(\frac{\Delta g}{\upsilon^2} \right)^{\frac{1}{3}} d$, d is the particle diameter and $\Delta = \frac{\rho_s}{\rho_w} - 1$

Regarding m, Richardson and Zaki (1954) proposed m=4.65 for laminar flow and Re > 500, m=2.39; however, as summarized by Chien and Wan (1999), several m values ranging from 1 to 7 have been proposed over the past couple of decades in which m values depends on the medium diameter of the particle as well. Therefore, the values range from the least of 2.25, considered by Mintz and Schubert (1958) to the highest value of 7 considered by Wang (2001). Yet a Sensitivity analysis revealed that changing the m parameter had only a limited influence on the outcome under the current situation, and m was given a value of 2.5 in this study. The additional CFX command language (CCL) function of the inflow discharge or velocity distribution and volumetric fraction were programmed as Dirichlet type in this study into the boundary setting. The simulation fluid was assumed to be isothermal and incompressible. The boundary conditions of the bed and wall were set to be a no-slip condition. The outlet flux was set according to the experimental model or reservoir operation, and the free surface was a rigid-lid approximation.

2.2.Model calibration and verification using flume data

Turbidity current venting simulations using laboratory data for model calibration Before model calibration, the accuracy of simulated result depending on coarse or fine mesh can be estimated by relative error (Lee et al., 2014). Therefore, before determining the grid size of the computational mesh in CFX model validation with experimental data, several types of grid sizes were tried to analyze the effect of mesh refinement.

The experimental flume was conducted in a 1 m long, 0.05 m wide, and 0.35 m deep glass-walled flume for the mesh analysis and model calibration. The slope of the flume bottom was adjustable and set to be horizontal as the topographic terrain in front of the dam of Zengwen Reservoir. A head tank with a mechanical stirrer was equipped to keep inflow sediment particles homogeneous in suspension. The suspended sediment mixture was supplied to the upstream end of the flume by controlling the valve, which created the sediment-laden flow moving toward the downstream outlet. At the end wall of the flume, a bottom outlet dimension of 0.05 m in width and 0.002 cm in height was installed and controlled by valves. To maintain steady water surface elevation in the flume, excessive supply water without disturbing the flow field was drained through an overflow weir at the downstream end of the flume. Compared with various simulation meshes, the computational mesh of 1/10 bottom outlet diameter reveals sufficient accuracy and consumed less CPU time. Therefore, the referenced computational mesh is adapted for followed model calibration and application cases. Since the equations are solved at cell (nodal) positions, a mesh is critical to the accuracy of the numerical solution. Therefore, the domain must be accurately and efficiently divided into discrete cells. The total number of nodes is 23100, and the total number of elements is 17928. The mesh is hexahedral throughout the geometry. The mesh is made denser near the region close to the bed and the outlet since it's essential to analyze the turbidity currents. The inflow boundary condition as Dirichlet type was given by a vertical distribution of unit width discharge and sediment concentration at the entrance section, and the max. inflow concentrations are given as 7000 ppm (case 1) and 9000ppm (case 2). At the outflow boundaries, zero normal velocity gradient and hydrostatic pressure distribution were imposed at the overflow weir, and measured outflow discharges were given at the bottom outlet openings. The water surface was approximated as a rigid-lid boundary in modelling. It means that the free surface was treated as a surface of symmetry of all variables, and the initial surface atmosphere pressure was set to be zero (De Cesare et al., 2006, Lee et al, 2014). The sediment concentration and fluid velocity are set to be 0 in the initial state of flume. The water balance in the CFX numerical model was solved by satisfying the continuity equation. From the simulated results, the turbidity current arrives at the bottom outlet first due to stratification of the suspension and clear water. In addition, when compared with the measured results, the simulated results show consistency and follow the trend.

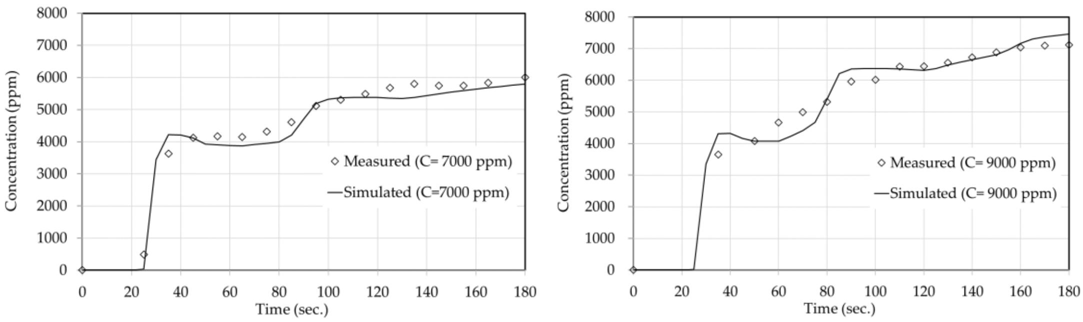

Figure 1. Sediment outflow concentration through outlet (a)inflow concentration is 7000ppm (b) inflow concentration is 9000ppm

After the turbulence model is chosen, the next step is to calibrate the parameter of viscosity coefficient (*a*) in Eq. (5). Different values for coefficient *a* ranging from 0.75 to 2.5 were tested. The value of 1 showed the least RMSE, and it can be seen in Figure 4 that by increasing the value of coefficient *a* beyond 1, the RMSE further increases. The calibrated values of coefficient *a* in this study are close to the value resulting from previous research value, 0.67, reviewed by Van Rijn (1987) and Sabine Chamoun et al. (2018).

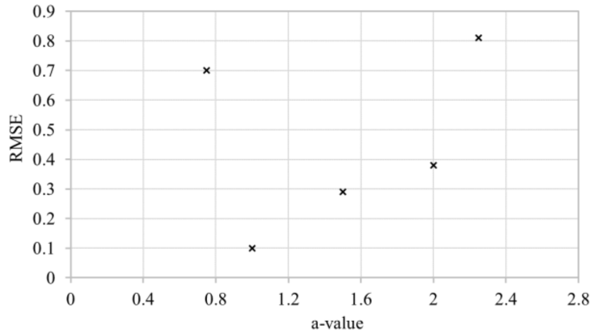

Figure 2. Root mean square (RMSE) in a-value of mixture dynamic viscosity.

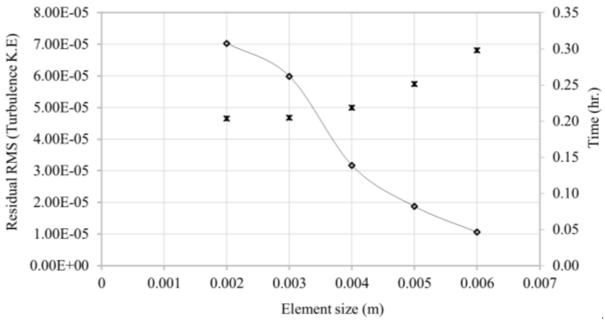

Figure 3. Mesh element size relation with RMSE and simulation time.

2.3.Numerical model verification using physical model and field data

After evaluating the model's credibility in simulating the turbidity current in a flume, we moved on to the simulations of turbidity currents during typhoon events in the Zengwen reservoir. In turbidity current simulations, experimental data for the event of typhoon Morakot from the Water Resource Agency (Southern District Taiwan) is used to calibrate the numerical model. Several sensitivity tests were conducted before achieving satisfactory numerical results. Different parameters, i.e., fall velocity, turbulence model, turbulent intensity, dynamic viscosity, and sediment characteristics, were used as significant model inputs.

2.3.1. Simulation of typhoon Morakot using physical model data

Typhoon Morakot was selected for model calibration and experiment data were obtained from the Office of Water Resource Agency (WRA)- Southern District, Taiwan. During Morakot, the peak discharge occurred at hour 45.8 and reached 10520 m^3/sec. In addition, the inflow volume of sediment was 64.45 M tons. Figure 4 (a) and (b) displays the inflow discharge hydrograph along with water level and inflow concentration respectively at Dapu station that were used as the inlet boundary conditions. Figure 4(b) shows the outflow discharge hydrograph of the reservoir outlets which are used as the outflow boundary conditions. The total simulated time was 100 h and model results were discussed and compared with the measured results below.

One of the most crucial components is the turbidity current movement speed; therefore, the comparison of simulated arrival time at different cross-sections to the experimental measurements has been made. The upstream boundary is located at 15,095 m at A-22. From A-21 (14,125 m) to A-01 (150 m), we measured arrival time data at 21 sections and plotted them in Figure 4 (d). The current arrived at section A-15 in 1.2 hours; the corresponding simulated time was 1.3 hours, a discrepancy of around 7.6 percent; at A-10, the arrival time was 2.83 h measured and 3 hours simulated (6.6 percent difference), at A-05 5.13 h measured and 5.25 hours simulated (2.28 percent difference). However, the highest discrepancy of 30% was observed for arrival time to A-01. The experimental data used is of the scaled physical model. Still, the particle size had not been scaled down during the experiments resulting in the lag of the arrival time from A-05 to A-01 due to a decrease in the velocity.

A model to predict outflow concentration through reservoir outlets is crucial as the amount of sediment vented through a reservoir outlet is an essential component for reservoir management. Since we evaluated the model credibility based on comparing outflow concentration in the flume, the same has been done for the model case. Outflow concentration over time through the desilting tunnel and the bottom outlet has been plotted in figure 4(c). It took 37 h for the current to arrive at the bottom outlet, while the corresponding model prediction was 34.5 h, a difference of about 6.75%. In comparison, it took 38.5 h for the current to arrive at the desilting tunnel, while the corresponding model prediction was 35 h, a difference of about 9.09%. The turbidity arrival time and front velocity are the are the essential characteristics. The arrival time could be identified by the outflow sediment concentration, which presented an abrupt rising tendency of records up to 22666 ppm for the bottom outlet; then the concentration value continuously rose and reached the peak outflow concentration of 85520 ppm. Whereas for the desilting tunnel, the abrupt rise of 23593 ppm outflow concentration was observed which, reaching the peak concentration of 79500 ppm. The measured peak outflows for the bottom outlet and desilting tunnel are 97300 ppm and 96500 ppm, respectively, with a difference of 12.1% and 17.61% from the simulated results, respectively.

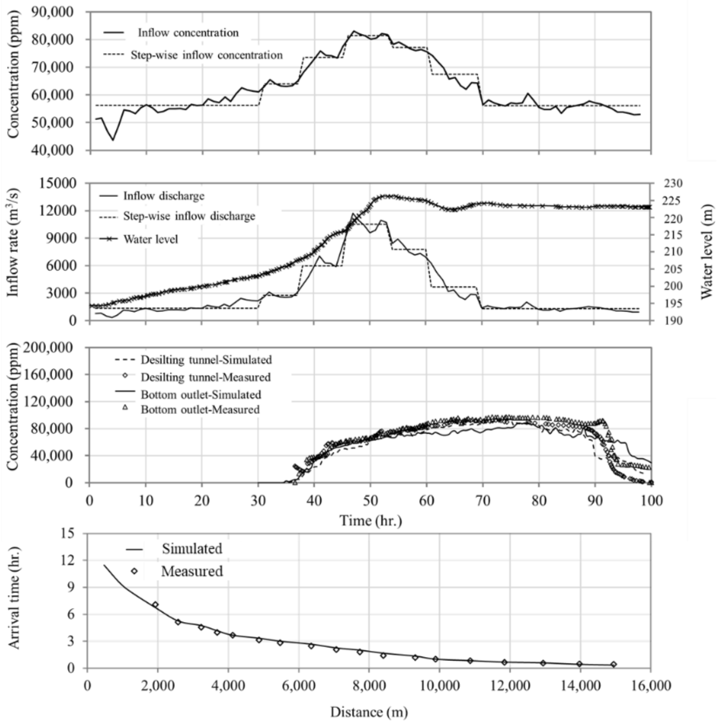

Figure 4. Hydrograph of (a) Inflow discharge and water level (b) Outflow discharge during and inflow concentration Typhoon Morakot (c) Outflow concentration through reservoir outlets (d) Arrival time of turbidity current

One of the most important variables for reservoir management during typhoon event is the venting efficiency (V.E) which can be calculated using expression developed by Morris & Fan (1998) given as

$$V.E = \frac{m_{out}}{m_{in}} = \frac{\sum_{i=0}^{T}(C_{out_i} Q_{out_i})}{\sum_{i=0}^{T}(C_{in_i} Q_{in_i})} \quad (7)$$

Where m_{out} and m_{in} , represent the masses of outflow and inflow sediments respectively, C_{out_i} and C_{in_i} are the respectively suspended sediment concentrations of outflow and inflow at time i, Q_{out_i} and Q_{out_i} are the respective outflow and inflow discharges at time i. As the Q_{in}/Q_{out} ratio increases so does the efficiency of venting. In practice, the timing and arrangement of gate openings at the dam have a significant impact on venting efficiency.

The simulated and the measured total venting efficiency are 25.5% and 31.36 %, respectively, with a total difference of 5.86%. Through each outlet, the measured and simulated venting efficiency are as follows: 5.63% and 4.97 %, respectively, for the spillway with a difference of 0.66%; for the bottom outlet, 4.96% and 2.98 %, respectively, with a difference of 1.98%; for desilting tunnel 19.85% and 17.55% respectively with a difference of 2.3%.

Simulated results show consistency with the measured result. Hence, proving our model is capable of testing the proposed reservoir management strategy.

2.3.2. Simulation of typhoon Lupit using field data

In August 2021, Tropical Storm Lupit skirted the east coast of China as it moved into the Taiwan Strait. Typhoon Lupit poured intermittent and potentially heavy rains throughout Taiwan's western part from south to north. Therefore, to verify our model, we simulated this case, and the measured data was acquired from the WRA, Southern office. An inflow discharge hydrograph and inflow sediment concentration hydrograph are set as boundary conditions for the inlet, as shown in Figure 5(a). Comparison of the measured and simulated outflow concentration for the bottom outlet, spillway and desilting tunnel are presented in figure 5(b).

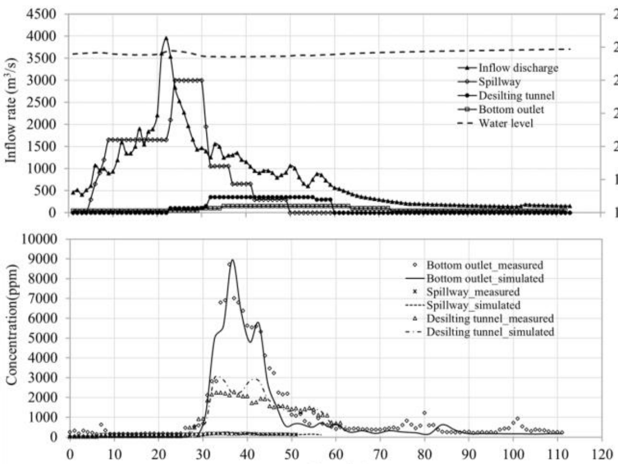

Figure 5. Hydrograph of (a) Inflow discharge and water level (b) Outflow concentration during Typhoon Lupit

Figure 6 (a-e) compares measured and simulated suspended sediment concentrations near the Zengwen dam at five sampling locations throughout elevation for typhoon Lupit. The measured data shows the stratified flow phenomenon of turbid density current while it approaches the dam, which the numerical model likewise well simulated. The arrival time of the turbidity current at the intake structure was measured to be 28 h which was similar to the simulated turbidity current. According to the measured data and simulated results, the peak sediment concentration at EL. 173 m recorded at 33 hours. After the turbidity current arrives at the intake structure, it will strike the intake structure and move upwards, eventually forming a submerged muddy lake until the end of the flooding period. After the turbidity current strikes the structure due to the loss of energy as well as a decrease in the inflow discharge and concentration, the suspended sediments will start to settle owing to the settling velocity of the sediment this phenomenon can be clearly observed in Figure 6. We observe that by employing the numerical model, the characteristics of the stratified flow phenomenon in the turbidity current generated during the typhoon Lupit were simulated well. Further, the comparison between the simulated and measured data was made in terms of the outflow concentration, which is presented in Figure 5(b).

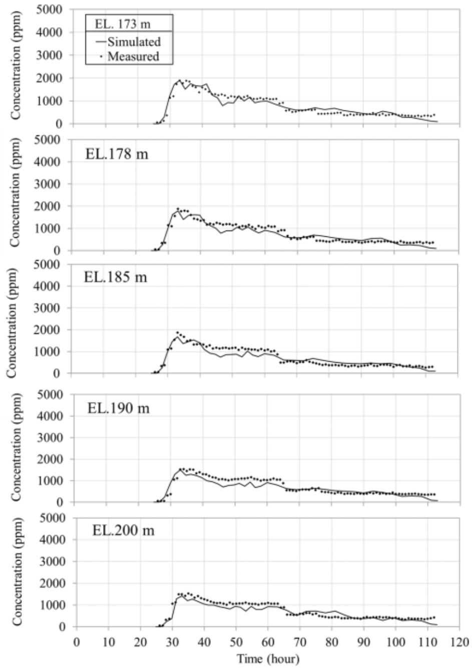

Figure 6. Comparison of measured and simulated suspended sediment concentration near dam site during typhoon Lupit (a) E.L. 173 m (b) E.L. 178 m (c) E.L. 185 m (d) E.L.190 m (e) E.L. 200 m

3. Model application

3.1 Reservoir management technique by introducing a dredged guiding channel

Among many globally tested techniques, the sediment routing techniques have proven the most effective in reducing reservoir sedimentation and maintaining or re-establishing sediment continuity similar to pre-dam conditions. Sediment routing is a concept that refers to a group of techniques that take advantage of the time-wise variation in sediment discharge to manage flows during periods of peak sediment yield in order to avoid sediment trapping in the reservoir. Moreover, these existing techniques can be modified and combined with other approaches to build up a single efficient method, which can potently tackle the presented challenge. Therefore, to come up with the sediment management strategy that is beneficial during typhoon events and dry seasons.

Therefore, testing one such technique involving dredging a guiding channel on the reservoir bed can help guide the turbidity currents generated during the flood events towards the reservoir outlets. We modified our reservoir geometry by constructing a guiding channel of depth 5m and width 200 m at the bottom bed of the reservoir from A-1 to A-10 cross-section. From A-10 to A-8 cross-section, the turbidity current takes a turn, and at such events, it could be seen that there was a slight decrease in the velocity. Due to the decline in the velocity, deposition chances are higher if the currents generated are short-lived.

According to previous studies, the front velocity of the turbidity current determines the distance that the current can reach and the time the current arrives at a certain point. As a result, turbidity currents created during flood occurrences can be confined in the excavated channel, reducing sediment dissipation at the cross-section where velocity decreases owing to a change in velocity streamline pattern. The path followed by the guiding channel is that of the flow velocity mainstream, whose location was obtained during the earlier simulations.

Our numerical study has considered three unsteady cases of peak flowrates 2769 m^3/sec, 4431 m^3/sec and 11840 m^3/sec with peak concentrations 36,719 mg/l, 57,374 mg/l and 1,45,856 mg/l respectively. The peak of 4431 m^3/sec is from the typhoon Jangmi which has a return period of five years. At the same time, 2.67 percent is added to the hydrograph of the five-year return period to obtain the hydrograph for the 100-year return period. Whereas to get the hydrograph for a return period of two years, the hydrograph of the five-year return period decreases by 1.6 percent.

3.2. Evaluation of dredged guiding channel in terms of Desilting efficiency

According to simulation results, the desilting efficiency of the desilting tunnel, bottom outlet, and spillway are 16.6%, 2.09 %, and 8.62 %, respectively, under the flow condition with a return period of 100 years. Applying the guiding channel model, the desilting efficiency of the outlets is 21.04 %, 5.17 %, and 11.22 % for the desilting tunnel, bottom outlet, and spillway, respectively. Thus, the difference in total desilting efficiency was 10.1 %.

The desilting efficiency of the desilting tunnel, bottom outflow, and spillway, according to simulation results, is 4.83 %, 0.24 %, and 0.006 %, respectively, under the flow condition with a 5-year return period. In comparison, the desilting efficiency of the outlets, computed using the guiding channel model, is 13.5 %, 1.35 %, and 1.204 % for the desilting tunnel, bottom outlet, and spillway, respectively. As a result, there was a 2.31% difference in total desilting efficiency of the two model simulations. From the simulated results, the sediment desilting efficiency of the desilting tunnel, bottom outflow, and spillway is 3.62 %, 0.08 %, and 0.001 %, respectively, under the flow condition with a 2-year return period. On the other hand, the guiding channel model simulations show that the desilting efficiency is 5.82 %, 0.13 %, and 1.006 % for the desilting tunnel, bottom outlet, and spillway, respectively. As a result, the total desilting efficiency of the two models differed by 3.05%. From the results mentioned above, the desilting efficiency increases when the guiding channel is considered irrespective of the inflow conditions.

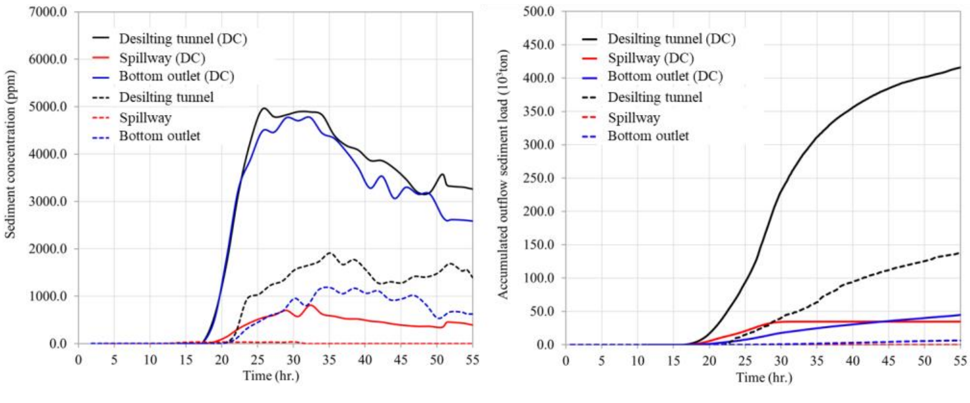

Figure 7. Simulated outflow concentration through reservoir outlets with inflow condition for return period of 5 years.

4. Conclusion

This study investigates the efficiency of a reservoir management technique of dredging a guiding channel and routing turbidity current towards reservoir outlets by evaluating the desilting efficiency through reservoir outlets. A 3D numerical model is used to simulate turbidity currents generated in the reservoir during typhoon events. For the calibration of the numerical model, data used was generated in the flume laboratory tests by Lee et al. (2014). At the same time, field data were obtained from WRA (Water Resource Agency), Taiwan, for model validation and verification.

Bottom outlets are critical release structures that can reduce the reservoir's level in an emergency, ensuring dam safety. If sediment clogs an outlet, it prevents it from being used and jeopardizes the safety of a dam. In addition, turbidity currents in some reservoirs can transport a large amount of sediment to the dam. In reservoirs, the combination of stratification and inflow can result in complex vertical profiles. According to the flume case of bottom outlets, the desilting efficiency is affected by flow mechanism, including discharges (active flow field), sediment concentration, and turbid thickness. Since the sediment concentrates near the reservoir bottom, the desilting efficiency of low-lying outlets is higher than elevated outlets. Therefore, 3D simulation is preferable for simulating stratified flow movement, i.e., turbidity current.

According to numerical findings, the model is competent in prophesying the characteristics influencing the turbidity current movement in the reservoir. Furthermore, it can predict the arrival time of the turbidity current, which can be seen to match adequately with the measured values. The model also accurately predicts the sediment desilting rates through all outlets. It is shown that the model can reasonably estimate sediment desilting rates through the desilting tunnel as well. The findings support the model's reliability in evaluating various desilting strategies.

The purpose of our study was to find a sustainable solution that will effectively slow down the sedimentation rate and increase the amount of sediment outflow through the reservoir outlets during typhoon events. A guiding channel was constructed in the model to concentrate the turbidity currents generated during floods within the channel and effectively vent these incoming sediments. Numerical findings show the guiding channel can concentrate the inflow of turbid water in the channel by minimizing sediment spread out. The guiding channel also increases the velocity of turbid water; therefore, turbidity current arrives early. To travel the long distances, the velocity of a turbid current must be sufficient enough to generate the turbulence required to maintain its sediment load in suspension thereby maintaining the density difference between the gravity-induced current and the surrounding fluid. Turbidity current having potential travel distance less than the length of reservoir may not be successful in passing through low level outlets in the dam. By considering a submerged guiding channel, the turbidity current velocity can be increased and the arrival time can be decreased as well. Further, the results show that dredging a guiding channel to increase the amount of desilting can prove helpful if implemented to tackle the sedimentation problem caused by typhoon events.

References

1. Wieland, M. Life-span of storage dams. 2010, 62, 32-35.
2. Wisser, D.; Frolking, S.; Hagen, S.; Bierkens, M.F.P. Beyond peak reservoir storage? A global estimate of declining water storage capacity in large reservoirs. Water Resources Research 2013, 49, 5732-5739.
3. Jodeau, M.; Chamoun, S.; Feng, J.; De Cesare, G.; Schleiss, A.J. Numerical Modeling of turbidity currents with Ansys CFX and Telemac 3D. E3S Web Conf. 2018, 40.

4. Morris, G.; Fan, J. Reservoir sedimentation handbook : design and management of dams, reservoirs, and watersheds for sustainable use. 1998.
5. Annandale, G.W.A.M., Gregory Karki, Pravin. Extending the Life of Reservoirs: Sustainable Sediment Management for Dams and Run-of-River Hydropower.
6. Chamoun, S.; De Cesare, G.; Schleiss, A.J. Managing reservoir sedimentation by venting turbidity currents: A review. International Journal of Sediment Research 2016, 31, 195-204.
7. Sastre, V.; Loizeau, J.-L.; Greinert, J.; Naudts, L.; Arpagaus, P.; Anselmetti, F.; Wildi, W. Morphology and recent history of the Rhone River Delta in Lake Geneva (Switzerland). Swiss Journal of Geosciences 2010, 103, 33-42.
8. Parker, G.; García, M.H.; Fukushima, Y.; Yu, W. Experiments on turbidity currents over an erodible bed. Journal of Hydraulic Research 1987, 25, 123-147.
9. Cesare Giovanni, D.; Schleiss, A.; Hermann, F. Impact of Turbidity Currents on Reservoir Sedimentation. Journal of Hydraulic Engineering 2001, 127, 6-16.
10. Lee, H.; Kim, E.; Park, S.; Choi, J. Effects of Climate Change on the Movement of Turbidity Flow in a Stratified Reservoir. Water Resources Management 2015, 29.
11. Lee, H.-Y.; Lin, Y.-T.; Chiu, Y.-J. Quantitative Estimation of Reservoir Sedimentation from Three Typhoon Events. Journal of Hydrologic Engineering 2006, 11, 362-370.
12. Chamoun, S.; Cesare, G.D.; Schleiss, A.J. Influence of Operational Timing on the Efficiency of Venting Turbidity Currents. Journal of Hydraulic Engineering 2018, 144, 04018062.
13. Wildt, D.; Hauer, C.; Habersack, H.; Tritthart, M. CFD Modelling of Particle-Driven Gravity Currents in Reservoirs. Water 2020, 12, 1403.
14. Wang, K.; Yang, J.-C.; Wu, C.H. 3D Modeling of Flood Induced Flows and Sediment Concentration in Shihmen Reservoir. 2008.
15. Lee, F.-Z.; Lai, J.-S.; Tan, Y.-C.; Sung, C.-C. Turbid density current venting through reservoir outlets. KSCE Journal of Civil Engineering 2014, 18, 694-705.
16. Georgoulas, A.; Angelidis, P.; Panagiotidis, T.; Kotsovinos, N. 3D Numerical modelling of turbidity currents. Environmental Fluid Mechanics 2010, 10, 603-635.
17. Kassem, A.; Imran, J. Simulation of turbid underflow generated by the plunging of a river. Geology 2001, 29.
18. Heimsund, S.; Hansen, E.; Nemec, W. Computational 3D fluid-dynamics model for sediment transport, erosion and deposition by turbidity currents; 2002.
19. Lavelli, A.; Boillat, J.; Cesare, G.D. Numerical 3D modelling of the vertical mass exchange induced by turbidity currents in Lake Lugano (Switzerland). 2002.
20. Cantero, M.; i, M.; Buscaglia, G. Multidimensional CFD simulation of a discontinuous density current. 2003.
21. Wu, B.; Wang, G.; Xia, J. Case Study: Delayed Sedimentation Response to Inflow and Operations at Sanmenxia Dam. Journal of Hydraulic Engineering-asce - J HYDRAUL ENG-ASCE 2007, 133.
22. Hung, M.-C.; Hsieh, T.; Wu, C.; Yang, J.-C. Two-Dimensional Nonequilibrium Noncohesive and Cohesive Sediment Transport Model. Journal of Hydraulic Engineering-asce - J HYDRAUL ENG-ASCE 2009, 135.
23. Wang, K.H.; Yang, J.-C.; Wu, C. 3D Modeling of Flood Induced Flows and Sediment Concentration in Shihmen Reservoir. Journal of Coastal Research 2008, 10052, 71-78.
24. Oehy, C.D.; Schleiss, A.J. Control of Turbidity Currents in Reservoirs by Solid and Permeable Obstacles. Journal of Hydraulic Engineering 2007, 133, 637-648.
25. Oehy, C.; De Cesare, G.; Schleiss, A. Effect of inclined jet screen on turbidity current. Journal of Hydraulic Research 2010, 48.

26. Goodarzi, D.; Lari, K.S.; Alighardashi, A. A large eddy simulation study to assess low-speed wind and baffle orientation effects in a water treatment sedimentation basin. Water Science and Technology 2018, 2017, 412-421.
27. Liu, W.-C.; Liu, H.-M.; Chiu, C.-Y. Investigating suspended-sediment transport in a shallow lake using a three-dimensional hydrodynamic and sediment model. Journal of Earth System Science 2019, 128.
28. Hillebrand, G.; Klassen, I.; Olsen, N.R.B. 3D CFD modelling of velocities and sediment transport in the Iffezheim hydropower reservoir. Hydrology Research 2017, 48, 147-159.
29. Huang, C.-C.; Lin, W.-C.; Ho, H.-C.; Tan, Y.-C. Estimation of Reservoir Sediment Flux through Bottom Outlet with Combination of Numerical and Empirical Methods. Water 2019, 11, 1353.
30. Rubey, W.W. The size distribution of heavy minerals within a water-laid sandstone. Journal of Sedimentary Research 1933, 3, 3-29.
31. Richardson, J.F.; Zaki, W.N. The sedimentation of a suspension of uniform spheres under conditions of viscous flow. Chemical Engineering Science 1954, 3, 65-73.
32. Chien, N.; Wan, Z. Fall Velocity of Sediment Particles. In Mechanics of Sediment Transport; 1999; pp. 63-114.
33. Camenen, B. Simple and General Formula for the Settling Velocity of Particles. Journal of Hydraulic Engineering 2007, 133, 229-233.
34. Zhiyao, S.; Tingting, W.; Fumin, X.; Ruijie, L. A simple formula for predicting settling velocity of sediment particles. Water Science and Engineering 2008, 126.
35. Engelund, F.; Hansen, E. A monograph on sediment transport in alluvial streams; Teknisk forlag: Copenhagen, 1972.